

AUSCULTABASE: A FOUNDATIONAL STEP TOWARDS AI-POWERED BODY SOUND DIAGNOSTICS

Pingjie Wang^{1,3}, Zihan Zhao^{1,3}, Liudan Zhao², Miao He⁴, Xin Sun², Ya Zhang^{1,3}
Kun Sun², Yanfeng Wang^{1,3}, Yu Wang^{1,3*}

¹ Shanghai Jiao Tong University

² Xinhua Hospital Affiliated To Shanghai Jiao Tong University School of Medicine

³ Shanghai Artificial Intelligence Laboratory

⁴ Tongji University

{pingjiewang, yuwangsjtu}@sjtu.edu.com

ABSTRACT

Auscultation of internal body sounds is essential for diagnosing a range of health conditions, yet its effectiveness is often limited by clinicians’ expertise and the acoustic constraints of human hearing, restricting its use across various clinical scenarios. To address these challenges, we introduce **AuscultaBase**, a foundational framework aimed at advancing body sound diagnostics through innovative data integration and contrastive learning techniques. Our contributions include the following: First, we compile **AuscultaBase-Corpus**, a large-scale, multi-source body sound database encompassing 11 datasets with 40,317 audio recordings and totaling 322.4 hours of heart, lung, and bowel sounds. Second, we develop **AuscultaBase-Model**, a foundational diagnostic model for body sounds, utilizing contrastive learning on the compiled corpus. Third, we establish **AuscultaBase-Bench**, a comprehensive benchmark containing 16 sub-tasks, assessing the performance of various open-source acoustic pre-trained models. Evaluation results indicate that our model outperforms all other open-source models in 12 out of 16 tasks, demonstrating the efficacy of our approach in advancing diagnostic capabilities for body sound analysis.

1 INTRODUCTION

Auscultation, the clinical skill of listening to internal body sounds, is essential for diagnosing a variety of health conditions. By analyzing heart sounds, respiratory sounds, and bowel sounds, clinicians can derive critical insights into a patient’s physiological state, enabling the monitoring of conditions such as valvular heart disease, congenital heart defects, pneumonia, asthma, gastroenteritis, and intestinal obstruction. However, the efficacy of auscultation is largely contingent upon the clinician’s expertise and the acoustic range of the human ear, which limits its application in various clinical scenarios (Mangione & Nieman, 1997). Recently, the integration of artificial intelligence algorithms for sound analysis has emerged as a promising approach to enhance diagnostic accuracy (Chen et al., 2023; Kong et al., 2020; Oletic & Bilas, 2017; Zhang et al., 2024; Sitaula et al., 2022).

Despite the progress made with existing methodologies, several challenges persist. First, while some approaches utilize general acoustic techniques to extract audio features from specialized stethoscope recordings, they may not adequately capture the pathological variations in body sounds (Chen et al., 2023; Guo et al., 2023; Oletic & Bilas, 2017; Jung et al., 2021). With advancements in unsupervised training, neural networks have been shown to effectively learn high-quality representations directly from audio data (Baevski et al., 2020; Huang et al., 2022; Hsu et al., 2021b; Wu et al., 2023). Some methods have proposed the use of these pretrained audio models for feature extraction for body sound (Koike et al., 2020; Panah et al., 2023). However, existing pretrained models are typically trained on general audio datasets like AudioSet (Gemmeke et al., 2017) and LibriSpeech (Panayotov et al., 2015) which contain sounds—such as music and speech—that significantly differ from those collected by stethoscopes, leading to substantial domain gaps that render them unsuitable for auscultation feature

*Corresponding Author.

extraction. Currently, there are publicly available datasets for the three types of body sounds and the details are shown in Tabel 1. Zhang et al. (2024) utilized publicly available respiratory sounds captured by stethoscopes alongside cough sounds recorded by microphones to develop respiratory sound representations. Baur et al. (2024) identified and utilized cough sounds, respiratory sounds, and laughter collected from YouTube to construct health-related acoustic representations. However, these methodologies are not specifically designed for auscultation and may not effectively adapt to the diverse range of body sounds captured by stethoscopes.

To address these critical gaps, we introduce **AuscultaBase**, a foundational framework designed to transform body sound diagnostics through advanced data integration and contrastive learning techniques. AuscultaBase offers a comprehensive solution that not only supports the diagnostic capabilities of primary care providers but also enables scalable, high-quality auscultation analysis, particularly for clinicians operating in high-volume, low-resource environments. Our framework is built upon three core pillars:

- **AuscultaBase-Corpus**: A Large-Scale, Multi-Source Body Sound Database. This extensive corpus combines 10 publicly accessible datasets and one private dataset, covering a diverse array of body sounds—heart, respiratory, and gastrointestinal—for a total of 322.4 hours of training recordings. The AuscultaBase-Corpus provides a rich, representative data foundation to train and evaluate diagnostic models across multiple auscultation systems.
- **AuscultaBase-Model**: A Foundational Diagnostic Model for Body Sounds. We developed a robust foundational model tailored for body sound diagnostics using contrastive learning techniques on the AuscultaBase-Corpus. This model captures nuanced acoustic patterns, showing significant improvements in diagnostic accuracy over conventional acoustic models. It offers a unified approach to analyzing different body sounds, setting a new standard for accuracy and reliability in auscultation.
- **AuscultaBase-Bench**: A Comprehensive Benchmark for Auscultation Evaluation. To facilitate rigorous assessment, AuscultaBase-Bench provides a structured evaluation framework across three primary diagnostic tasks—abnormality detection, disease classification, and activity recognition—spanning 16 sub-tasks that reflect the diverse and complex demands of clinical auscultation. This benchmark enables consistent, standardized performance comparisons for current and future auscultation models.

2 RELATED WORKS

The auscultatory body sounds include heart sounds, respiratory sounds, and bowel sounds. Existing models typically focus on one specific type of body sound. For heart sounds, the primary tasks concentrate on abnormal detection and disease diagnosis. Most methods employ traditional acoustic features for feature processing. For example, Chen et al. (2023) initially applied noise reduction to the audio and then utilized Short-Time Fourier Transform (STFT) to obtain the audio spectrogram. Their main network was constructed using a CNN and included an attention module at the end. Guo et al. (2023) combined high-order spectral estimation with STFT for audio feature extraction and designed a dual-stream CNN as the primary network. Some approaches have also introduced general audio pre-training models, such as the study that compared the effectiveness of features extracted using PANN (Kong et al., 2020) with those derived from non-pre-trained models using STFT features alongside architectures like VGG and ResNet, demonstrating the transferable capabilities of general audio pre-training models in the field of heart sound diagnosis (Koike et al., 2020).

For respiratory sounds, the tasks are similarly focused on abnormal detection and disease diagnosis. Early methods employed traditional feature extraction techniques such as STFT and MFCC (Oletic & Bilas, 2017; Jung et al., 2021). In recent years, due to the COVID-19 pandemic, several pre-training models targeting respiratory sounds have emerged. Zhang et al. (2024) utilized cough sound data collected via microphones and respiratory sound data obtained from stethoscopes to construct a pre-training dataset, comparing two contrastive methods and one generative method, demonstrating the efficacy of the pre-training model across 19 tasks involving cough and respiratory sounds. Baur et al. (2024) developed a health acoustic event detector that identifies audio clips from YouTube corresponding to specific events, including coughing, breathing, throat clearing, laughing, and speaking, followed by pre-training using a generative approach based on MAE (He et al., 2022), and subsequently fine-tuning on downstream tasks related to the identified events.

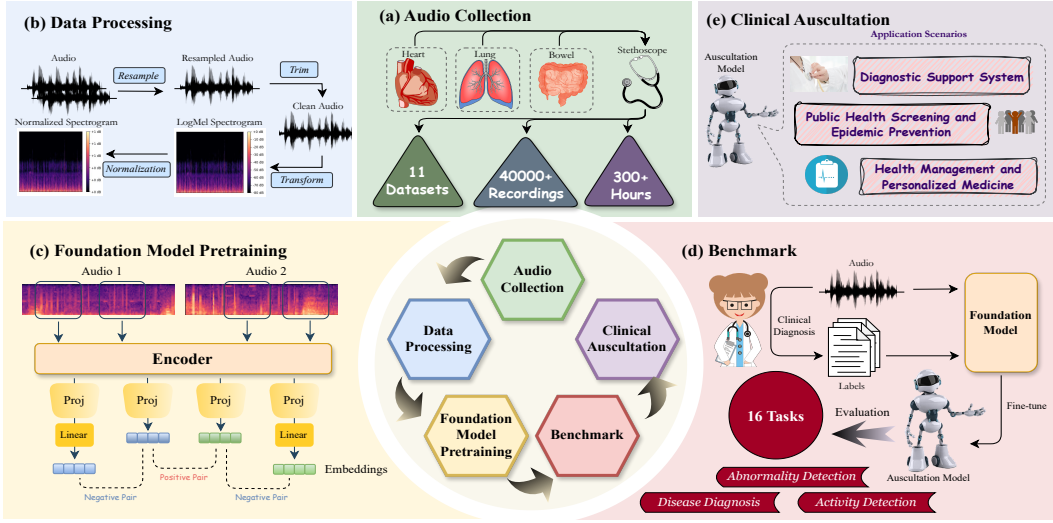


Figure 1: System overview of AuscultAbase. The AuscultAbase-Corpus is first collected by (a) Audio Collection and then processed by (b) Data Processing. AuscultAbase-Model is obtained by (c) Foundation Model Pretraining and evaluated with AuscultAbase-Bench: (d) Benchmark. Based on the tasks, the fine-tuned model can be applied for various scenarios of (e) Clinical Auscultation.

Regarding bowel sounds, there is a relative lack of datasets and methods, with the primary task being bowel sound detection. Among them, most methods have been tested on proprietary datasets. Sitaula et al. (2022) first collected bowel sound data from 49 newborns and constructed a model combining CNN with Laplace’s hidden semi-markov model after extracting audio features using MFCC. Baronetto et al. (2023) collected bowel sound data from 18 participants and explored the effects of using Audioset for pre-training, along with various CNN and attention-based architectures.

Existing methods overlooked the interrelatedness of various body sounds in auscultation, focusing exclusively on individual categories of sounds. In contrast, the proposed A4Body-Model fully considers this correlation by utilizing all data related to auscultation for pre-training. In this way, our approach meets the high data requirements for pre-training while eliminating the potential noise impact from unrelated audio.

3 SYSTEM OVERVIEW

The system overview of **AuscultAbase** is exhibited in Figure 1, which consists of three main components: pretraining datasets (-Corpus), foundation model(-Model), and evaluation benchmark (-Bench). Firstly, the -Corpus is curated by the collection of existing body sound datasets and then processed (Section 4) for subsequent pretraining the -Model as elaborated in Section 5. Then the -Bench is introduced to evaluate existing models comprehensively including 16 tasks in Section 6.

4 AUSCULTABASE-CORPUS: PRETRAINING DATASETS

11 datasets are collected to curate AuscultAbase-Corpus and enable the pretraining of our auscultation model, which involves lung, heart, and bowel sounds (shown in Table 1). After filtering the broken audio clips, the entire pertaining datasets consist of 40, 317 samples, with a total duration of 322.4 hours. All of them can be publicly available except for HSDreport and XHheartSound, in which XHheartSound is a private dataset collected by Xinhua Hospital Affiliated To Shanghai Jiao Tong University School of Medicine and has not been open source yet. All of them were made with different versions of digital stethoscopes attached to the chest, heart, and bowel respectively. This allows our model to acquire more powerful capabilities for identifying the frequency and beat of the body sounds, and then better boosting the application to clinical auscultation. It is noted that some

Dataset	Sound Type	SR	#Sample	Duration (s)	Total (h)
SPRSound (Zhang et al., 2022)	L	8kHz	3554	11.2 [0.3~15.4]	11.0
HF Lung (Hsu et al., 2021a)	L	4kHz	13957	15.0 [15.0~15.0]	58.2
ICBHI 2017 (Rocha et al., 2019)	L	4~44.1kHz	920	21.5 [7.9~86.2]	5.5
Lung Sound (Fraivan et al., 2021)	L	4kHz	336	17.4 [5.0~30.0]	1.6
Respiratory Database@TR (Altan et al., 2017)	L	4kHz	504	21.7 [14.8~30.0]	3.0
Korean (Yaseen et al., 2018)	H	8kHz	1000	2.4 [1.2~4.0]	0.7
Cinc 2016 (Clifford et al., 2016)	H	2kHz	3240	22.5 [5.3~122.0]	20.2
Circor 2022(Oliveira et al., 2021)	H	4kHz	3163	22.9 [5.2~64.5]	20.1
HSDReport (Zhao et al., 2024)	H	4~8kHz	3660	63.1 [6.9~132.7]	64.2
XHheartSound	H	4~8kHz	8377	59.0 [1.5~132.7]	137.0
Bowel Sound (Ficek et al., 2021)	B	44.1kHz	1606	2.0 [2.0~2.0]	0.9
Total	-	-	40317	-	322.4

Table 1: Statistics of the pretraining datasets (SR: sampling rate; Duration: mean [min, max]), where the sound type is categorized into lung (L), heart (H), and bowel (B) sounds.

of the labeled samples are held out from the pertaining datasets, which can be used for subsequent downstream benchmarking.

Table 1 demonstrates the statistics of our pretraining datasets. As the data sources vary such as in the auscultation position, sampling rate, and durations, we first resample each recording to 16kHz and merge them into a mono channel. After that, the beginning and ending silence is removed to ensure the quality of the recordings. The trimmed clips are then transformed using 64 LogMel Spectrogram with a Hanning window which shifts every 32 ms. The spectrograms are then standardized with Min-Max Normalization and finally used to pretrain our auscultation foundation model.

5 AUSCULTABASE-MODEL: AUSCULTATION FOUNDATION MODEL

We utilize the aforementioned combination of datasets in Table 1 to pre-train our auscultation model. For the datasets that have been split into training and validation sets, we reserve the validation ones as our validation sets. For others, we shuffle the samples and randomly select 10% for validation.

As the result of the nature of body sounds, the recordings of them usually share similar patterns. Therefore, to make the model distinguish the nuances among recordings and capture the abnormality of each audio, we adopt the contrastive learning-based objective to pre-train our model. Specifically, two segments from the same recording are regarded as positive pairs, otherwise negative pairs. The rationale behind this choice is that if an encoder can capture nuances among different sources, it is expected to encode recognizable and generalizable acoustic features for downstream evaluation.

To adapt to the varied length of recordings as exhibited in Table 1, we refer to Chen et al. (2022) and utilize a transformer-based network as the encoder to extract features. Then a projector is adopted to map the features into a lower dimension, and the bilinear similarity will be calculated among obtained low-dimensional representations. The optimization objective aims to maximize the similarity between positive pairs and minimize it for negative pairs. Specifically, due to inherent variations in audio length within an individual batch, we employ random cropping to obtain segments for training. To guarantee the difficulty of the optimization target, we construct a separate dataloader for each dataset and ensure the audio clips from each batch are from the same dataset. The batches are sampled from different data loaders randomly.

The cropped length is set as 320 ms for Korean and Bowel Sound while other datasets share the length of 640 ms. We project the encoded representations into a 512-dimensional space and the model for 200 epochs. We employ an Adam optimizer with a learning rate of 1e-4 which decayed by 0.99 every one epoch.

ID	Dataset	Sound Type	Task Type	Class Name	Data Distribution
T1	SPRSound	L	MC	Normal / Adventitious / Poor Quality	2324 / 1000 / 230
T2	SPRSound	L	MC	Normal / CAS / DAS / CAS&DAS / Poor Quality	2324 / 368 / 480 / 152 / 230
T3	HF Lung	L	BC	Normal / Abnormal	52444 / 29489
T4	HF Lung	L	MC	Inhalation / Exhalation / CAS / DAS	34095 / 18349 / 13883 / 15606
T5	HF Lung	L	MC	Inhalation / Exhalation / Wheeze / Stridor / Rhonchi / Crackle	34095 / 18349 / 8457 / 686 / 4740 / 15606
T6	ICBHI 2017	L	MC	Normal / Crackle / Wheeze / Crackle&Wheeze	3642 / 1864 / 886 / 506
T7	Lung Sound	L	MC	Normal / Crepitation / Wheeze / Crackle / Bronchi / Wheeze&Crackle / Bronchi&Crackle	105 / 69 / 123 / 24 / 3 / 6 / 6
T8	Circor 2022	H	MC	Present / Absent / Unknown	363 / 2391 / 156
T9	ICBHI 2017	L	MC	Healthy / Bronchiectasis / Bronchiolitis / COPD / Pneumonia / URTI	35 / 16 / 13 / 793 / 37 / 23
T10	Lung Sound	L	ML	Normal / Asthma / Pneumonia / COPD / BRON / Heart failure / Lung fibrosis / Pleural effusion	105 / 99 / 15 / 33 / 9 / 63 / 18 / 6
T11	Respiratory Database@TR	L	MC	COPD0 / COPD1 / COPD2 / COPD3 / COPD4	72 / 60 / 84 / 84 / 204
T12	Korean	H	MC	Normal / Aortic Stenosis / Mitral Regurgitation / Mitral Stenosis / Murmur in Systole	200 / 200 / 200 / 200 / 200
T13	Cinc 2016	H	BC	Normal / Abnormal	2575 / 665
T14	Circor 2022	H	BC	Normal / Abnormal	1632 / 1531
T15	HSDReport	H	BC	Normal / Abnormal	247 / 2028
T16	Bowel Sound	B	R	-	0~43

Table 2: Downstream task characteristics grouped by function category (T1-T8: abnormality detection, T9-T15: disease diagnosis, T16: activity detection). The task type is categorized into binary classification (BC), multi-class classification (MC), multi-label classification (ML), and regression (R) tasks. Data Distribution represents the numerical range of the frequency of bowel sounds for T16, while for T1-T15 it denotes the number of samples corresponding to the class names.

6 AUSCULTABASE-BENCH: AUSCULTATION BENCHMARK

To assess the auscultation capability of existing auscultation foundation models, we construct Auscultabase-Bench, a novel benchmark on all the datasets we have collected as shown in Table 1. It is noted that we have previously excluded all the test sets in the pertaining state to avoid data leakage.

6.1 TASKS

Our benchmark consists of a total of 16 tasks involving binary classification, multi-class classification, multi-label classification, and regression, as demonstrated in Table 2. We assort these tasks by their function as abnormality detection, disease diagnosis, and activity detection tasks.

Abnormality Detection tasks (T1-T8) aim to distinguish whether the body sound is normal and which normality or abnormality it belongs to. For example, T8 targets to identify if any murmur exists in the heart sound, while T4 requires the model to identify whether the patient is inhaling or exhaling and whether the adventitious sounds are continuous (CAS) or discrete (DAS) if they exist. The abnormality of body sounds may indicate unusual health conditions but still require clinicians to confirm and report the diagnosis.

Disease Diagnosis tasks (T9-T15) focus on distinguishing if the patient is healthy and which disease the patient may suffer from. For example, T12 aims to distinguish whether the heart sound is healthy or reveals any symptoms of cardiac diseases. T11 requires models to identify the level of chronic obstructive pulmonary disease (COPD) which ranges from 0 to 4. It is noted that we exclude “LRTI” and “Asthma” from the original dataset for T9 because The sample proportions for these two categories are rather small and do not appear in the test set. These tasks require the auscultation

	OPERA-CT	AudioMAE	CLAP	PANN	AusculptaBase-Model
# Parameters (M)	31	86	80	82	31
Feature Dim.	768	768	1024	2048	768
# Samples (K)	136	2000	128	1934	40
Total Duration (h)	440	5000+	~250	5000+	322

Table 3: Comparison of existing acoustic pre-trained models and AusculptaBase-Model.

model to integrate the entire recording to analyze if any diagnosis exists instead of focusing on local details. Moreover, these tasks provide specific disease diagnoses rather than symptoms that require clinical confirmation.

Activity Detection task (T16) targets evaluating the frequency of a specific activity or pattern. T16 evaluates the bowel function by counting the frequency of bowel sounds within a recording.

6.2 BASELINES

OPERA-CT (Zhang et al., 2024) is a contrastive learning-based pre-trained model for respiratory audio feature extraction. As the first respiratory acoustic foundation models, OPERA family models leverage quantities of breathing and cough sounds to conduct pertaining and demonstrate superior performance and generalizability against existing acoustic models pre-trained with general audio. We select OPERA-CT, the most powerful with the largest number of parameters as the baseline.

AudioMAE (Huang et al., 2022) is a self-supervised pre-trained model for audio understanding, inspired by the Masked Autoencoders (MAE) (He et al., 2022) approach used in vision tasks. It works by randomly masking portions of the audio signal during pre-training and learning to reconstruct the missing parts. This method allows the model to capture meaningful audio features without requiring labeled data. AudioMAE has shown strong performance across various audio classification and sound event detection tasks.

CLAP (Elizalde et al., 2023) is a language-supervised pre-trained model that bridges the gap between audio and natural language through contrastive learning. By training on paired audio and text data, CLAP learns to align audio features with corresponding textual descriptions, enabling cross-modal retrieval and classification. This approach enhances the model’s capability to interpret and relate audio content with high-level semantic information, making it a robust baseline for audio-linguistic tasks.

PANN (Kong et al., 2020) is a convolutional neural network designed for audio pattern recognition, pre-trained on large-scale datasets for audio tagging and sound event detection. It achieves high accuracy in detecting environmental sounds, musical instruments, and other acoustic events. Its architecture is specifically tailored for efficient feature extraction from audio signals, making it a strong baseline for various audio analysis tasks. More comparisons about the number of parameters, feature dimensions, the number of overall samples, and total durations of recordings in the pretraining datasets are detailed in Table 3.

6.3 BENCHMARKING PROTOCOL

All tasks are evaluated using the standard linear probe protocol, which freezes the pre-trained audio encoder and only trains a single fully connected layer on top of the encoded representations. Such a protocol focuses on the quality and generalizability of the encoded features and avoids the overfitting problem with a small dataset. It is noted that we adopt different data pre-processing strategies (e.g. resampling and feature extraction) for different baselines strictly following their own official implementations. As for our foundation model, the same audio pre-processing procedures are applied as in the pertaining stage. Due to the significant variation in audio lengths (e.g. 5.3~122.0 s for Cinc 2016), we split all the training set audio into equal-length segments for training. We finetune the linear head for 64 epochs with a decayed learning rate of $1e-4$ by default.

Function	ID	Sound Type	Task Type	OPERA-CT	AudioMAE	CLAP	PANN	AusculptaBase-Model
Abnormality Detection	T1	L	MC	45.41±1.95	38.19±1.19	48.05±0.43	26.01±0.06	48.36 ±0.16
	T2	L	MC	26.20±1.09	19.77±3.01	36.42 ±0.10	15.54±0.02	30.28±3.11
	T3	L	BC	46.51±1.38	55.58±0.05	55.07±0.58	40.99±0.00	56.00 ±1.63
	T4	L	MC	33.60 ±0.26	28.15±1.15	33.01±0.21	17.04±0.32	33.09±1.76
	T5	L	MC	22.76±0.09	19.08±1.10	22.41±0.55	11.19±0.14	23.45 ±0.46
	T6	L	MC	29.63±1.39	24.66±3.47	37.61 ±0.30	34.92±0.01	29.61±0.19
	T7	L	MC	36.14±1.09	27.38±6.85	34.39±5.37	11.07±0.14	42.61 ±1.87
	T8	H	MC	44.01±1.39	41.69±2.29	47.49 ±4.16	28.71±0.00	39.93±0.16
Disease Diagnosis	T9	L	MC	22.30±3.23	21.04±1.91	35.79 ±9.32	24.79±3.40	31.16±0.10
	T10	L	ML	20.94±0.33	20.45±0.00	20.30±0.58	20.45±0.00	20.97 ±0.21
	T11	L	MC	31.46±5.22	11.83±0.00	31.69±4.05	31.45±6.85	41.54 ±3.44
	T12	H	MC	77.93±1.38	55.35±6.74	86.21±2.05	87.52±2.48	88.71 ±0.32
	T13	H	BC	66.99±1.55	73.72±1.75	64.87±1.34	65.56±0.60	76.38 ±1.24
	T14	H	BC	60.44±1.74	57.42±4.26	60.35±0.35	48.17±0.23	62.10 ±0.82
	T15	H	BC	51.02±3.75	47.27±0.00	51.02±3.75	47.27±0.00	64.96 ±2.22

Table 4: Macro-F1 scores for abnormality detection (T1-T8) and disease diagnosis (T9-T15) tasks. The best model for each task is in **bold**. We report mean and standard deviation with 3 runs.

Function	ID	Sound Type	Task Type	OPERA-CT	AudioMAE	CLAP	PANN	AusculptaBase-Model
Abnormality Detection	T1	L	MC	69.41±1.37	64.18±0.75	72.59±0.69	63.65±0.03	72.71 ±0.25
	T2	L	MC	64.80±0.31	63.77±0.16	65.73±0.56	63.61±0.00	66.11 ±0.69
	T3	L	BC	70.18±0.28	68.98±0.46	67.06±2.62	69.45±0.00	71.15 ±0.04
	T4	L	MC	53.08 ±0.20	49.62±0.12	48.93±0.29	49.61±0.00	51.91±0.31
	T5	L	MC	51.66±0.52	49.47±0.21	48.85±0.02	49.63±0.02	51.77 ±0.16
	T6	L	MC	47.31±1.67	42.41±16.04	56.22±0.92	58.49 ±0.94	51.78±5.15
	T7	L	MC	50.00±4.54	40.91±10.01	46.97±7.58	24.24±0.00	59.10 ±1.52
	T8	H	MC	77.53±0.32	79.75±0.63	81.49 ±0.48	75.63±0.00	78.49±0.31
Disease Diagnosis	T9	L	MC	91.33±0.27	91.60 ±0.00	87.27±5.64	91.50±0.37	91.60 ±0.26
	T10	L	ML	22.41±0.50	23.32 ±1.10	22.63±1.58	22.80±0.58	22.88±0.88
	T11	L	MC	38.00±2.00	42.00±0.00	45.00±1.00	43.00±3.00	50.00 ±2.00
	T12	H	MC	77.50±1.50	56.00±8.00	86.50±2.50	87.50±2.50	88.50 ±0.50
	T13	H	BC	83.23±0.31	81.99±0.62	82.14±0.16	78.11±1.09	86.50 ±0.47
	T14	H	BC	61.39±0.95	59.65±5.22	60.76±0.63	55.70±0.00	63.29 ±0.63
	T15	H	BC	89.87±0.21	89.66±0.00	89.87±0.22	89.66±0.00	90.52 ±0.00

Table 5: Micro-F1 scores for abnormality detection (T1-T8) and disease diagnosis tasks (T9-T15). The best model is in **bold**, and the mean and standard deviation are reported with 3 runs.

6.4 METRIC

Macro-F1 and **Micro-F1** are reported respectively for each classification task to evaluate the performance across classes and samples. We report both of them because the Macro-F1 scores reflect the model’s ability to handle classes equally well, irrespective of class size, while the Micro-F1 scores emphasize overall classification accuracy across all classes. For the regression task, the **Accuracy** is computed. Additionally, **AUROC** (Area Under the Receiver Operating Characteristic) is calculated for binary classification tasks and **Class-wise F1** scores for each class are reported for multi-class classification tasks. For a comprehensive overall evaluation, we also report the **MRR** (Mean Reciprocal Rank) scores and **BSC** (Borda Count Score) of performance categorized by different perspectives.

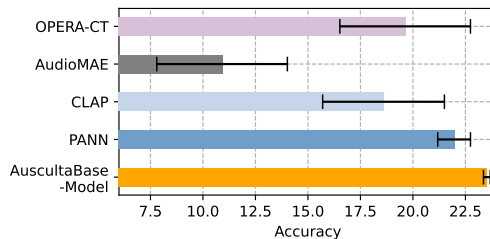


Figure 2: Accuracy scores for the activity detection task. The best model is in **bold**, and the error bars are reported with 3 runs.

Metric	Function	#	OPERA-CT	AudioMAE	CLAP	PANN	AuscultaBase-Model
Macro-F1	Abnormality Detection	8	0.4688	0.2854	0.6042	0.2375	0.6875
	Disease Diagnosis	7	0.3571	0.2571	0.4381	0.3024	0.9286
	Overall	15	0.4167	0.2722	0.5267	0.2678	0.8000
Micro-F1	Abnormality Detection	8	0.4583	0.2854	0.4292	0.3396	0.7708
	Disease Diagnosis	7	0.3426	0.4500	0.3262	0.3071	0.8571
	Overall	15	0.4044	0.3622	0.3811	0.3244	0.8111
Accuracy	Activity Detection	1	0.3333	0.2000	0.2500	0.5000	1.0000

Table 6: Mean reciprocal ranks (MRR) grouped by functions and evaluation metrics. The best model within each group is in bold. # means the number of tasks of each group.

7 RESULTS

7.1 COMPREHENSIVE RESULTS OVERVIEW

The Macro-F1 and Micro-F1 scores for abnormality detection (T1-T8) and disease diagnosis (T9-T15) tasks are exhibited in Table 4 and 5, while the accuracy for the activity detection (T16) task is shown in Figure 2.

Consistent Superiority. The results in Table 4, 5, and Figure 2 demonstrate that our proposed AuscultaBase-Model outperforms baseline models across various tasks. Specifically, our model attains the top performance on 10 tasks for Macro-F1 and 11 tasks for Micro-F1 out of 15 classification tasks. In contrast, other baselines only achieve superior results on individual tasks. For instance, PANN delivers the highest score only once for the Micro-F1 score (T6) but never achieves the best for the Macro-F1 score. Notably, our model consistently achieves higher performance across various body sounds like lung, heart, and bowel sounds, indicating its superior capability in capturing distinctive and generalizable acoustic features for body sounds.

Balance in Performance. AuscultaBase-Model achieves a more balanced performance in both Macro-F1 and Micro-F1 scores, which is crucial for classification tasks, especially those involving imbalanced datasets. To evaluate the model’s balanced performance across both metrics, we focus on tasks where the best results were achieved simultaneously for both Macro-F1 and Micro-F1. We find that only 11 tasks (T1, T3-T5, T7-T8, T11-T15) have a model that reaches optimal performance in both metrics. Among these, our model achieves the best results in 9 tasks, while OPERA-CT and CLAP each lead in one task. This balanced optimization is crucial in practical applications, particularly in domains involving imbalanced datasets, where strong performance across all metrics is essential to ensure both minority and majority classes are well-represented.

7.2 CATERGORIZED COMPARISON

To provide a broader understanding of the models’ overall effectiveness across various tasks and domains, we categorize these tasks from different perspectives: function, sound type, and task type. Then we adopt MRR (Mean Reciprocal Ranks) and BCS (Borda count scores) metrics of the reported Macro-F1 scores to conduct a comprehensive analysis for them.

Function. In the function perspective analysis, we compute the MRR across tasks. As shown in Table 6, AuscultaBase-Model consistently achieves the highest MRR in both abnormality detection and disease diagnosis tasks, significantly outperforming other baseline models. Specifically, in disease diagnosis, our model achieved an MRR of 0.9286 for Macro-F1, whereas other models lagged behind, highlighting our model’s capability to not only detect general abnormalities but also make precise and nuanced clinical assessments. This distinction is critical in practical medical applications where the identification of specific diseases can directly impact patient care and treatment decisions. The superior performance of our model across these functions signifies its robustness and precision in both the detection of abnormalities and accurate disease classification, making it particularly valuable for healthcare diagnostics.

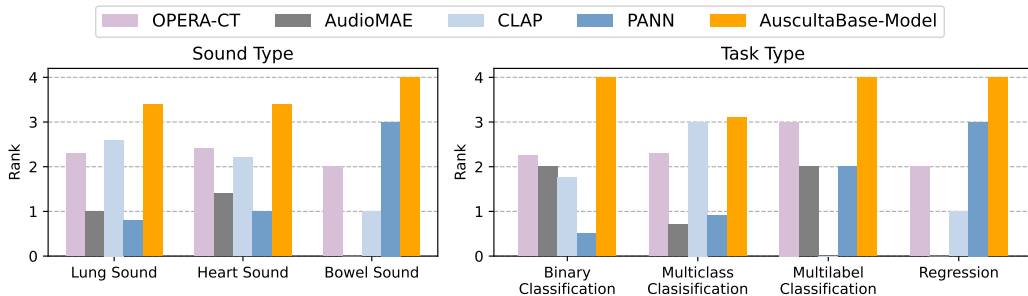


Figure 3: Borda count scores (BCS) scores categorized by the sound type (left) and task type (right).

ID	Sound Type	OPERA-CT	AudioMAE	CLAP	PANN	AuscultaBase-Model
T3	L	0.643±0.004	0.573±0.002	0.643±0.001	0.507±0.000	0.645±0.005
T13	H	0.875±0.001	0.872±0.004	0.859±0.001	0.831±0.002	0.917±0.003
T14	H	0.606±0.018	0.635±0.003	0.628±0.007	0.540±0.002	0.659±0.020
T15	H	0.790±0.007	0.694±0.022	0.776±0.336	0.576±0.004	0.802±0.006

Table 7: The AUROC of binary classification tasks (T3, T13-T15). The best results for each task across different auscultation models are in bold.

Sound Type. In the sound type analysis, we evaluate the performance of each model using the BCS of their Macro-F1 scores for lung sound, heart sound, and bowel sound tasks. As demonstrated in Figure 3, our Auscultabase-Model ranks the highest overall, especially excelling in bowel sound tasks. As shown in the left panel of the figure, our model consistently achieves the best performance across different sound types, demonstrating its ability to handle diverse and complex acoustic environments. This strong adaptability makes our model particularly effective for a wide range of body sound classification scenarios.

Task Type. For the analysis of task type, which includes binary classification, multi-class classification, multi-label classification, and regression, our model also performs exceptionally well. The right panel of Figure 3 shows that our model consistently achieves top performance across all task types especially for binary classification tasks, suggesting a high degree of flexibility and robustness. This is especially important for ensuring that the model can effectively generalize to different problem formulations, ranging from straightforward binary classification to complex multi-label scenarios and regression.

7.3 AUROC FOR BINARY CLASSIFICATION

To further assess the discriminative power of each model in binary classification tasks, we calculate the AUROC for the binary classification tasks (T3, T13, T14, and T15). Unlike metrics like the F1 score, AUROC provides a more comprehensive evaluation by measuring the model’s ability to distinguish between positive and negative classes at different thresholds.

As shown in Table 7, our model consistently outperforms the other baselines across all tasks, demonstrating its superior capability to distinguish between healthy and abnormal states effectively. For instance, in T13 (heart sound classification), our model achieves an AUROC of 0.917, which is notably higher compared to the best baseline OPERA-CT (0.875). These results underscore the robustness of our model when dealing with challenging binary classification problems, especially those involving subtle variations in body sounds. The results show that our model can effectively capture the critical features necessary for distinction, providing a reliable tool for medical diagnostic applications. This consistent superiority across multiple binary classification tasks highlights the overall generalizability and effectiveness of our model in real-world healthcare scenarios.

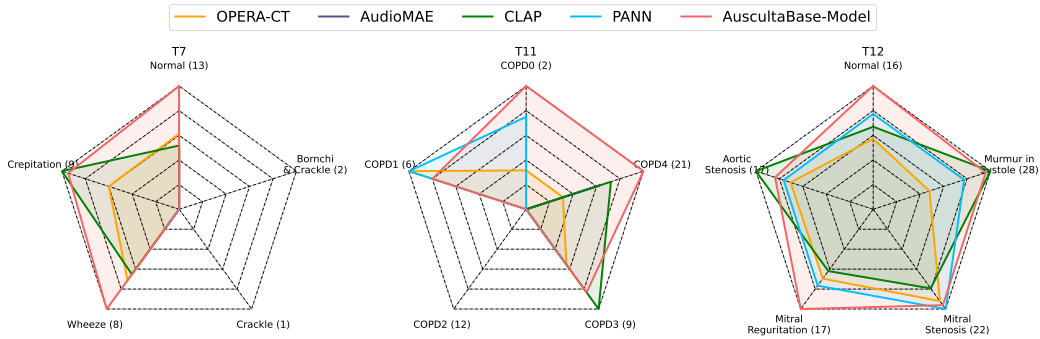


Figure 4: Class-wise F1 scores for multi-class classification tasks (T7, T11, T12). Each label at the corner of the radar chart represents a category, with the number in parentheses indicating the count of samples of that category within the test set. We exclude classes “Bronchi” and “Wheeze&Crackle” for T7 because they are not represented in the test set.

ID	#	Method	OPERA-CT	AudioMAE	CLAP	PANN	AuscultaBase-Model
T13	2918	Linear	0.875±0.001	0.872±0.004	0.859±0.001	0.831±0.002	0.917±0.003
		Full	0.961±0.007	0.951±0.007	0.857±0.003	0.959±0.006	0.978±0.003
T15	3294	Linear	0.790±0.007	0.694±0.022	0.776±0.336	0.576±0.004	0.802±0.006
		Full	0.784±0.001	0.760±0.063	0.776±0.004	0.652±0.037	0.824±0.013

Table 8: AUROC for linear probing and full fine-tuning on T13 and T15. # represents the number of training samples for the task.

7.4 CLASS-WISE PERFORMANCE FOR MULTI-CLASS TASKS

Building upon the previous evaluations which present a comprehensive analysis, this section aims to delve deeper into how each model handles individual classes, especially under imbalanced conditions. To this end, we plot the F1 scores of different models on multi-class classification tasks (T7, T11, T12) using radar charts. To make a clearer comparison, the results for each class are applied with Min-Max normalization across different models. As shown in Figure 4, our model (depicted in red) consistently shows superior or competitive F1 scores across both majority and minority classes.

For example, in T7 (which is highly imbalanced as shown in Table 2), our model achieves higher scores for the minority categories such as “Crepitation” and “Wheeze”, indicating its capability to effectively learn meaningful features even from underrepresented classes. This balanced performance across categories, irrespective of their distribution, highlights our model’s robustness and effectiveness in dealing with skewed datasets.

For T11, which involves classifying the severity of COPD, the class distribution is also significantly imbalanced, with “COPD4” having a much higher number of samples compared to “COPD0” and “COPD1”. Despite this challenge, Figure 4 indicates that our model still achieves high F1 scores not only in the majority class (“COPD4”) but also in minority classes like “COPD0”, suggesting that our model can handle class imbalance effectively without overly favoring majority classes. This indicates a good generalization capability and adaptability in identifying underrepresented classes.

Similarly, for T12, although the overall and test set distributions are more balanced across classes (e.g., each class has around 200 samples and shares a balanced number of test samples), our model still achieves superior F1 scores in multiple categories. This suggests that our model not only excels in imbalanced scenarios but also maintains superiority when the class distribution is relatively uniform.

7.5 FULL FINE-TUNING PERFORMANCE

In this section, we highlight the performance of different models under full finetuning, focusing on both binary and multi-class classification tasks. For binary tasks such as T13 and T15, Table 8 depicts that our model consistently achieves the highest AUROC scores after full finetuning. Specifically, on

ID	#	Metric	Method	OPERA-CT	AudioMAE	CLAP	PANN	AusculptaBase-Model
T11	454	Macro-F1	Linear	31.46±5.22	11.83±0.00	31.69±4.05	31.45±6.85	41.54 ±3.44
			Full	45.04±2.97	48.48±0.97	32.87±7.27	53.01±8.63	55.14 ±4.01
		Micro-F1	Linear	38.00±2.00	42.00±2.00	45.00±1.00	43.00±3.00	50.00 ±2.00
			Full	49.00±3.00	54.00±3.00	47.00±1.00	54.00±8.00	57.00 ±5.00

Table 9: Macro-F1 and Micro-F1 scores for linear probing and full finetuning on T11.

T13, our model reached an AUROC of 0.978, which makes it highly effective for clinical applications that require accurate identification of specific conditions.

For the multi-class classification task T11 as shown in Table 9, which features a relatively small number of training samples (454), our model demonstrates notable improvements after full finetuning, achieving a Macro-F1 of 55.14 and a Micro-F1 of 57.00. The performance gain over linear finetuning suggests that our model is highly adaptable, effectively capturing complex class relationships even when training data is limited. This adaptability is crucial for real-world medical diagnostics, where imbalanced datasets and limited data availability are common challenges. Our model’s ability to excel under such conditions further underscores its robustness and utility in various healthcare scenarios.

8 CONCLUSION

This work presents a large-scale body sound corpus (A4Body-Corpus), an auscultation acoustic foundation model (A4Body-Model), and a comprehensive benchmark for evaluation (A4Body-Bench). Our work addresses existing limitations in traditional auscultation practices through the integration of AI. By training on a diverse collection of body sounds using contrastive learning, our model shows a substantial improvement over existing pre-trained acoustic models, especially in imbalanced and limited-data settings. The full fine-tuning results reveal the robustness of our model in both binary and multi-class classification tasks, underscoring its potential for real-world clinical applications. This work emphasizes the value of combining traditional auscultation with AI-driven methods to deliver more reliable and accessible healthcare solutions, paving the way for the broader adoption of AI in medical diagnostics.

REFERENCES

- Gökhan Altan, Yakup Kutlu, Yusuf Garbi, Adnan Özhan Pekmezci, and Serkan Nural. Multimedia respiratory database (respiratorydatabase@ tr): Auscultation sounds and chest x-rays. *Natural and Engineering Sciences*, 2(3):59–72, 2017.
- Alexei Baevski, Yuhao Zhou, Abdelrahman Mohamed, and Michael Auli. wav2vec 2.0: A framework for self-supervised learning of speech representations. *Advances in neural information processing systems*, 33:12449–12460, 2020.
- Annalisa Baronetto, Luisa S Graf, Sarah Fischer, Markus F Neurath, and Oliver Amft. Segment-based spotting of bowel sounds using pretrained models in continuous data streams. *IEEE Journal of Biomedical and Health Informatics*, 27(7):3164–3174, 2023.
- Sebastien Baur, Zaid Nabulsi, Wei-Hung Weng, Jake Garrison, Louis Blankemeier, Sam Fishman, Christina Chen, Sujay Kakarmath, Minyoi Maimbolwa, Nsala Sanjase, et al. Hear–health acoustic representations. *arXiv preprint arXiv:2403.02522*, 2024.
- Junxin Chen, Zhihuan Guo, Xu Xu, Li-bo Zhang, Yue Teng, Yongyong Chen, Marcin Woniak, and Wei Wang. A robust deep learning framework based on spectrograms for heart sound classification. *IEEE/ACM Transactions on Computational Biology and Bioinformatics*, 2023.
- Ke Chen, Xingjian Du, Bilei Zhu, Zejun Ma, Taylor Berg-Kirkpatrick, and Shlomo Dubnov. Hts-at: A hierarchical token-semantic audio transformer for sound classification and detection. In *ICASSP 2022-2022 IEEE International Conference on Acoustics, Speech and Signal Processing (ICASSP)*, pp. 646–650. IEEE, 2022.

-
- Gari D Clifford, Chengyu Liu, Benjamin Moody, David Springer, Ikaro Silva, Qiao Li, and Roger G Mark. Classification of normal/abnormal heart sound recordings: The physionet/computing in cardiology challenge 2016. In *2016 Computing in cardiology conference (CinC)*, pp. 609–612. IEEE, 2016.
- Benjamin Elizalde, Soham Deshmukh, Mahmoud Al Ismail, and Huaming Wang. Clap: learning audio concepts from natural language supervision. In *ICASSP 2023-2023 IEEE International Conference on Acoustics, Speech and Signal Processing (ICASSP)*, pp. 1–5. IEEE, 2023.
- Jakub Ficek, Kacper Radzikowski, Jan Krzysztof Nowak, Osamu Yoshie, Jaroslaw Walkowiak, and Robert Nowak. Analysis of gastrointestinal acoustic activity using deep neural networks. *Sensors*, 21(22):7602, 2021.
- Mohammad Fraiwan, Luay Fraiwan, Basheer Khassawneh, and Ali Ibnian. A dataset of lung sounds recorded from the chest wall using an electronic stethoscope. *Data in Brief*, 35:106913, 2021.
- Jort F Gemmeke, Daniel PW Ellis, Dylan Freedman, Aren Jansen, Wade Lawrence, R Channing Moore, Manoj Plakal, and Marvin Ritter. Audio set: An ontology and human-labeled dataset for audio events. In *2017 IEEE international conference on acoustics, speech and signal processing (ICASSP)*, pp. 776–780. IEEE, 2017.
- Zhihuan Guo, Junxin Chen, Tongyue He, Wei Wang, Haider Abbas, and Zhihan Lv. DS-CNN: Dual-stream convolutional neural networks based heart sound classification for wearable devices. *IEEE Transactions on Consumer Electronics*, 2023.
- Kaiming He, Xinlei Chen, Saining Xie, Yanghao Li, Piotr Dollár, and Ross Girshick. Masked autoencoders are scalable vision learners. In *Proceedings of the IEEE/CVF conference on computer vision and pattern recognition*, pp. 16000–16009, 2022.
- Fu-Shun Hsu, Shang-Ran Huang, Chien-Wen Huang, Chao-Jung Huang, Yuan-Ren Cheng, Chun-Chieh Chen, Jack Hsiao, Chung-Wei Chen, Li-Chin Chen, Yen-Chun Lai, et al. Benchmarking of eight recurrent neural network variants for breath phase and adventitious sound detection on a self-developed open-access lung sound database—hf_lung_v1. *PLoS One*, 16(7):e0254134, 2021a.
- Wei-Ning Hsu, Benjamin Bolte, Yao-Hung Hubert Tsai, Kushal Lakhota, Ruslan Salakhutdinov, and Abdelrahman Mohamed. Hubert: Self-supervised speech representation learning by masked prediction of hidden units. *IEEE/ACM transactions on audio, speech, and language processing*, 29:3451–3460, 2021b.
- Po-Yao Huang, Hu Xu, Juncheng Li, Alexei Baevski, Michael Auli, Wojciech Galuba, Florian Metze, and Christoph Feichtenhofer. Masked autoencoders that listen. *Advances in Neural Information Processing Systems*, 35:28708–28720, 2022.
- Shing-Yun Jung, Chia-Hung Liao, Yu-Sheng Wu, Shyan-Ming Yuan, and Chuen-Tsai Sun. Efficiently classifying lung sounds through depthwise separable cnn models with fused stft and mfcc features. *Diagnostics*, 11(4):732, 2021.
- Tomoya Koike, Kun Qian, Qiuqiang Kong, Mark D Plumbley, Björn W Schuller, and Yoshiharu Yamamoto. Audio for audio is better? an investigation on transfer learning models for heart sound classification. In *2020 42nd Annual International Conference of the IEEE Engineering in Medicine & Biology Society (EMBC)*, pp. 74–77. IEEE, 2020.
- Qiuqiang Kong, Yin Cao, Turab Iqbal, Yuxuan Wang, Wenwu Wang, and Mark D Plumbley. Panns: Large-scale pretrained audio neural networks for audio pattern recognition. *IEEE/ACM Transactions on Audio, Speech, and Language Processing*, 28:2880–2894, 2020.
- Salvatore Mangione and Linda Z Nieman. Cardiac auscultatory skills of internal medicine and family practice trainees: a comparison of diagnostic proficiency. *Jama*, 278(9):717–722, 1997.
- Dinko Oletic and Vedran Bilas. Asthmatic wheeze detection from compressively sensed respiratory sound spectra. *IEEE journal of biomedical and health informatics*, 22(5):1406–1414, 2017.

-
- Jorge Oliveira, Francesco Renna, Paulo Dias Costa, Marcelo Nogueira, Cristina Oliveira, Carlos Ferreira, Alípio Jorge, Sandra Mattos, Thamine Hatem, Thiago Tavares, et al. The circor digiscope dataset: from murmur detection to murmur classification. *IEEE journal of biomedical and health informatics*, 26(6):2524–2535, 2021.
- Davoud Shariat Panah, Andrew Hines, and Susan McKeever. Exploring wav2vec 2.0 model for heart murmur detection. In *2023 31st European Signal Processing Conference (EUSIPCO)*, pp. 1010–1014. IEEE, 2023.
- Vassil Panayotov, Guoguo Chen, Daniel Povey, and Sanjeev Khudanpur. Librispeech: an asr corpus based on public domain audio books. In *2015 IEEE international conference on acoustics, speech and signal processing (ICASSP)*, pp. 5206–5210. IEEE, 2015.
- Daniel S Park, William Chan, Yu Zhang, Chung-Cheng Chiu, Barret Zoph, Ekin D Cubuk, and Quoc V Le. SpecAugment: A simple data augmentation method for automatic speech recognition. *arXiv preprint arXiv:1904.08779*, 2019.
- Bruno M Rocha, Dimitris Filos, Luís Mendes, Gorkem Serbes, Sezer Ulukaya, Yasemin P Kahya, Nikša Jakovljevic, Tatjana L Turukalo, Ioannis M Vogiatzis, Eleni Perantoni, et al. An open access database for the evaluation of respiratory sound classification algorithms. *Physiological measurement*, 40(3):035001, 2019.
- Jan Schlüter and Thomas Grill. Exploring data augmentation for improved singing voice detection with neural networks. In *ISMIR*, pp. 121–126, 2015.
- Chiranjibi Sitaula, Jinyuan He, Archana Priyadarshi, Mark Tracy, Omid Kavehei, Murray Hinder, Anusha Withana, Alistair McEwan, and Faezeh Marzbanrad. Neonatal bowel sound detection using convolutional neural network and laplace hidden semi-markov model. *IEEE/ACM Transactions on Audio, Speech, and Language Processing*, 30:1853–1864, 2022.
- Yusong Wu, Ke Chen, Tianyu Zhang, Yuchen Hui, Taylor Berg-Kirkpatrick, and Shlomo Dubnov. Large-scale contrastive language-audio pretraining with feature fusion and keyword-to-caption augmentation. In *ICASSP 2023-2023 IEEE International Conference on Acoustics, Speech and Signal Processing (ICASSP)*, pp. 1–5. IEEE, 2023.
- Yaseen, Gui-Young Son, and Soonil Kwon. Classification of heart sound signal using multiple features. *Applied Sciences*, 8(12):2344, 2018.
- Qing Zhang, Jing Zhang, Jiajun Yuan, Huajie Huang, Yuhang Zhang, Baoqin Zhang, Gaomei Lv, Shuzhu Lin, Na Wang, Xin Liu, et al. Sprsound: Open-source sjtu paediatric respiratory sound database. *IEEE Transactions on Biomedical Circuits and Systems*, 16(5):867–881, 2022.
- Yuwei Zhang, Tong Xia, Jing Han, Yu Wu, Georgios Rizos, Yang Liu, Mohammed Mosuily, Jagmohan Chauhan, and Cecilia Mascolo. Towards open respiratory acoustic foundation models: Pretraining and benchmarking. *arXiv preprint arXiv:2406.16148*, 2024.
- Zihan Zhao, Pingjie Wang, Liudan Zhao, Yuchen Yang, Ya Zhang, Kun Sun, Xin Sun, Xin Zhou, Yu Wang, and Yanfeng Wang. Hsdreport: Heart sound diagnosis with echocardiography reports. *arXiv preprint arXiv:2408.08669*, 2024.

CONTENTS

A Datasets	14
A.1 Datasets Availability	14
A.2 Datasets Description	15
B Demographic and Clinical Information	17
B.1 Age and Gender	17
B.2 Auscultation position	17
B.3 Sound Spectrogram	20
C Downstream Task Description	20
D Implementation Details	23
D.1 Pretraining	23
D.2 Benchmarking	23
E Pretraining Results	23
E.1 Pretraining Loss & Accuracy	23
E.2 Embedding Distribution	24
F Additional Evaluation Results	26
F.1 Performance Radar Plot	26

A DATASETS

A.1 DATASETS AVAILABILITY

We utilized 11 datasets in our benchmark, with access methods and licensing details provided in Table 10. A more detailed description of each dataset is provided below. Notably, all datasets include both audio recordings and accompanying metadata. The audio data has been anonymized, and the metadata contains no personally identifiable information or offensive content.

Dataset	Source	Access	License
SPRSound	SJTU	https://github.com/SJTU-YONGFU-RESEARCH-GRP/SPRSound	CC-BY-4.0
HF Lung	NTU	https://gitlab.com/techsupportHF/HF_Lung_V1	CC-BY-4.0
ICBHI 2017	*	https://bichallenge.med.auth.gr/ICBHI_2017_Challenge	CC0
Lung Sound	JUST&KAUH	https://data.mendeley.com/datasets/jwyy9np4gv/3	CC-BY-4.0
RespiratoryDatabase@TR	ITU	https://data.mendeley.com/datasets/p9z4h98s6j/1	CC-BY-4.0
Korean	SJU	https://github.com/yaseen21khan/Classification-of-Heart-Sound-Signal-Using-Multiple-Features-	CC-BY-4.0
Cinc 2016	*	https://archive.physionet.org/physiobank/database/challenge/2016/	Custom license
Circor 2022	*	https://physionet.org/content/circor-heart-sound/1.0.3/	ODC-By
HSDReport	SJTU	not available	-
XHheartSound	-	-	-
Bowel Sound	WUT&PUMS	https://www.kaggle.com/robertnowak/bowel-sounds	CC BY-NC 4.0

Table 10: Dataset availability. *The Cinc 2016, Circor 2022, and HF Lung datasets are derived from multiple sources, as detailed in the text descriptions below. The datasets presented in the HSDReport are not yet publicly available.

A.2 DATASETS DESCRIPTION

SPRSound (Zhang et al., 2022). The database is the first open-access pediatric respiratory sound database, jointly developed by Shanghai Jiao Tong University and its affiliated hospitals, with the aim of analyzing respiratory sounds in children. It comprises 2,683 recordings and 9,089 respiratory sound events from 292 participants, with a total duration of 11 hours. It includes annotations at both the event and record levels. At the event level, the distribution of sound types is as follows: Normal (6,887), Rhonchi (53), Wheeze (865), Stridor (17), Coarse Crackle (66), Fine Crackle (1,167), and Wheeze & Crackle (34). At the record level, the number of recordings categorized into Normal, Continuous Adventitious Sounds (CAS), Discrete Adventitious Sounds (DAS), CAS & DAS, and Poor Quality are 1,785, 233, 347, 131, and 187, respectively. The average duration of respiratory sound events and records is 1.3 seconds and 11 seconds, respectively. The sounds were recorded using a digital stethoscope (Yunting Model II) at four back locations: left posterior, left lateral, right posterior, and right lateral. Recordings at each location lasted over 9 seconds to capture at least two respiratory cycles (one cycle consisting of inhalation and exhalation).

HF Lung (Hsu et al., 2021a). This lung sound database was designed to facilitate the development of algorithms for detecting inhalation, exhalation, and adventitious lung sounds. The recordings originate from two primary sources. The first source is a database used during the 2020 Taiwan Smart Emergency and Critical Care (TSECC) datathon, licensed under the Creative Commons Attribution 4.0 (CC BY 4.0) license, and provided by the Taiwan Society of Emergency and Critical Care Medicine (TSECCM). This dataset includes lung sound recordings from 261 patients. The second source consists of recordings from 18 residents of a respiratory care ward (RCW) or respiratory care center (RCC) in Northern Taiwan, collected between August 2018 and October 2019. These recordings were approved by the Research Ethics Review Committee of Far Eastern Memorial Hospital (Case No. 107052-F), and written informed consent was obtained from all participants. The database contains 9,765 lung sound recordings, each 15 seconds in length, and includes corresponding labels: 34,095 inhalation labels, 18,349 exhalation labels, 13,883 continuous adventitious sound labels (8,457 wheeze, 686 stridor, 4,740 rhonchi), and 15,606 discontinuous adventitious sound labels (all classified as crackles). The database, HF_Lung_V1, developed by Heroic-Faith Medical Science Co. Ltd., is licensed under a Creative Commons Attribution 4.0 (CC BY 4.0) International License. All patients were Taiwanese and over 20 years of age.

ICBHI 2017 (Rocha et al., 2019). The International Conference on Biomedical and Health Informatics (ICBHI) 2017 database comprises 920 respiratory sound recordings from 126 participants, along with two sets of annotations. One set includes 6,898 annotated respiratory cycles, identifying the presence of crackles, wheezes, both, or no adventitious sounds. The second set provides detailed annotations for 10,775 crackle and wheeze events. The database contains audio samples independently collected by two research teams over several years in different countries, with ethical approval obtained from the relevant institutions. Most recordings were contributed by the Respiratory Research and Rehabilitation Laboratory (Lab3R) at the University of Aveiro, Portugal. These samples were gathered from various clinical settings, including Hospital Infante D. Pedro in Aveiro, Hospital Santa Maria and Lusíadas in Porto, and the University of Southampton, UK. Five separate studies from this team are represented, with recordings from the trachea and six chest locations (left and right anterior, posterior, and lateral) in both clinical and home environments. Participants ranged in age and included individuals with conditions such as lower and upper respiratory tract infections, pneumonia, COPD, asthma, bronchiolitis, bronchiectasis, and cystic fibrosis.

Lung Sound (Fraiwan et al., 2021). The dataset contains respiratory sound recordings from 112 subjects, including 35 healthy individuals and 77 with various respiratory conditions. The subjects' ages ranged in from 21 to 90 years, with a mean age of 50.5 ± 19.4 years, and the group comprises 43 females and 69 males. Each recording lasts between 5 and 30 seconds, which is sufficient to capture at least one full respiratory cycle. Lung sounds were recorded using an electronic stethoscope, with the stethoscope placement determined by a specialist physician. The dataset includes normal breathing sounds as well as sounds associated with seven conditions: asthma, heart failure, pneumonia, bronchitis, pleural effusion, lung fibrosis, and chronic obstructive pulmonary disease (COPD). Each recording was made three times, using different frequency filters to highlight various bodily sounds.

RespiratoryDatabase@TR (Altan et al., 2017). The RespiratoryDatabase@TR is a comprehensive database designed to facilitate the analysis of respiratory disorders. Developed by Iskenderun Technical University, Turkey. It includes lung and heart sounds, chest X-rays, pulmonary function test (PFT) data, and responses to the St. George Respiratory Questionnaire (SGRQ-C). These data were collected from patients at Antakya State Hospital using digital stethoscopes to capture lung sounds from 12 channels across the upper, middle, and lower lung regions, as well as the costophrenic angles. Heart sounds were recorded from four key areas: aortic, pulmonary, tricuspid, and mitral regions. The database, validated and labeled by two pulmonologists, categorizes subjects based on chest X-rays, PFT results, and auscultation findings, classifying them into five levels of COPD severity (COPD0 to COPD4). It includes both healthy individuals and patients with respiratory conditions such as asthma, COPD, and bronchitis, offering a broad spectrum of clinical insights into respiratory health.

Korean (Yaseen et al., 2018). The database, released by Sejong University, consists of two sets: a normal set and an abnormal set. It is further divided into five categories: one normal category (N) and four abnormal categories—aortic stenosis (AS), mitral stenosis (MS), mitral regurgitation (MR), and mitral valve prolapse (MVP). Each category contains 200 audio files, for a total of 1,000 files, all in ".wav" format. The data were collected from various sources, including auscultation skill CDs, heart sound educational materials, and 48 different websites (e.g., those from Washington, Texas, 3M, and Michigan). After removing files with excessive noise, the recordings were resampled to a frequency rate of 8,000 Hz and converted to mono channel, producing 3-period heart sound signals.

Cinc 2016 (Clifford et al., 2016). The PhysioNet/Computing in Cardiology (CinC) Challenge 2016 database was compiled from eight sources by seven research groups worldwide. It includes nearly 30 hours of recordings, comprising 4,430 heart sound recordings from 1,072 subjects. These recordings capture 233,512 heart sounds from both healthy individuals and patients with heart valve disease or coronary artery disease, with lengths varying from a few seconds to several minutes. The database also provides information on the subjects (age, gender), details about each recording (location on the body, duration), and additional signals such as ECG, along with data on sampling frequency and sensor type. Heart sounds are classified into three categories: normal (no need for further diagnosis), abnormal (needs further diagnosis), and unsure (too noisy to assess). The sounds are further labeled as normal for healthy subjects or abnormal for patients with heart conditions like valve defects or coronary artery disease, including cases like mitral valve prolapse and aortic stenosis.

Circor 2022 (Oliveira et al., 2021). This pediatric heart sound dataset was collected during two mass screening campaigns, called "Caravana do Coração" (Caravan of the Heart), conducted in the state of Paraíba, Brazil, in 2014 (CC2014) and 2015 (CC2015). Data collection was approved by the ethics board of the Complexo Hospitalar HUOC/PROCAPE, under the request of the Real Hospital Português de Beneficência. The dataset omprises 5,282 recordings from 1,568 participants with 50.2% male and 49.8% female, covering four main auscultation sites. The mean age of participants was 73.4 ± 0.1 months, ranging from 0.1 to 356.1 months. In total, 215,780 heart sounds were manually annotated, with 103,853 sounds (51,945 S1 and 51,908 S2) from CC2014 and 111,927 sounds (56,449 S1 and 55,478 S2) from CC2015. All participants completed socio-demographic questionnaires, followed by clinical examinations, nursing assessments, and cardiac investigations, including chest X-rays, electrocardiograms, and echocardiograms.

HSDReport (Zhao et al., 2024). The dataset consists of 2,275 participants under 18 years old of age, along with 2,275 auscultation recordings and corresponding echocardiography data. The authors later expanded the dataset to include a total of 3,660 samples. Heart sounds were recorded at five body sites: the aortic region (right 2nd intercostal space), pulmonic region (left 2nd intercostal space), Erb's point (left 3rd intercostal space), tricuspid region (left 4th intercostal space), and mitral region (left 5th intercostal space, midclavicular line). Each site was recorded for at least 15 seconds using an electronically amplified stethoscope (Littmann 3200, 3M) in direct contact with the skin. This study adhered to strict ethical standards, ensuring participant confidentiality and compliance with relevant regulations. Informed consent was obtained from all participants or their legal guardians, with a clear explanation of the study's purpose, the data to be collected (heart sounds and ultrasound reports), and its intended research use.

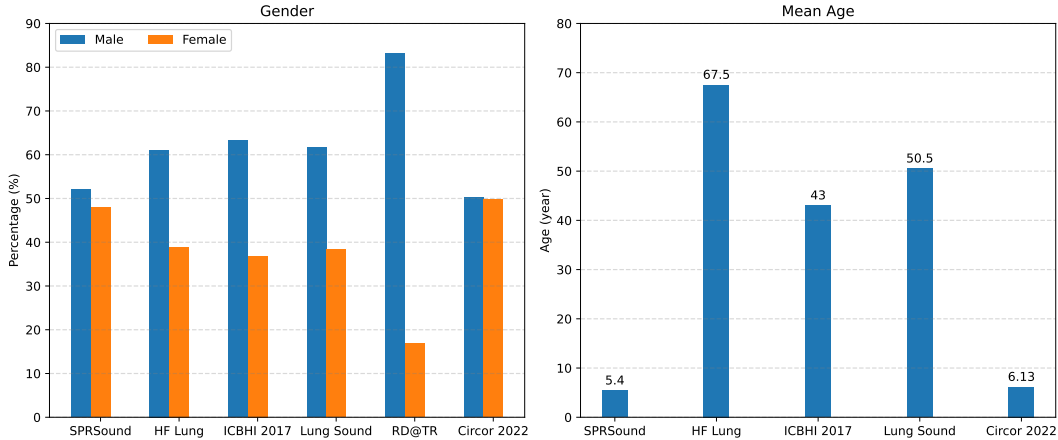


Figure 5: Gender distribution and mean age distribution for some of the datasets used in our benchmark.

XHheartSound. This dataset consists of 8,377 auscultation audios recorded by 8,377 children participants without diagnostic labels. The auscultation devices, positions, and procedures are followed with those of HSDReport. This research is carried out with a strong focus on ethics, protecting participant privacy, and following all rules. Before taking part, all individuals or their legal guardians were given full details about the study’s goals, what data would be collected (such as heart sounds and ultrasound results), and how this data would be used for research. Consent was obtained only after making sure everyone understood these details. This dataset is collected by Xinhua Hospital Affiliated To Shanghai Jiao Tong University School of Medicine, and due to the copyright constraint, it has not been open source yet.

Bowel Sound (Ficek et al., 2021). The dataset, released by Warsaw University of Technology, Warsaw University, and Poznań University of Medical Sciences, is a bowel sound dataset containing 321,000 recordings, each 10 milliseconds long and labeled by medical doctors. It includes nearly 100 recordings collected by a team from the Department of Pediatric Gastroenterology and Metabolic Diseases in Poznań, Poland. Recordings from 19 subjects were divided into 2-second fragments and then mixed. Of these, 15% were randomly selected as test data, while the remaining 85% were used for training and fivefold cross-validation.

B DEMOGRAPHIC AND CLINICAL INFORMATION

B.1 AGE AND GENDER

In our benchmark, we used a total of 10 datasets. The diversity and representativeness of the training data are crucial for developing a generalizable model. We examined the population distribution of the 10 datasets used for model pre-training. The bar charts in Figure 5 illustrate the gender distribution of 6 datasets and the mean age distribution of 5 datasets. Although the age distribution of the HSDReport dataset is unknown, it is known that all participants are children aged 18 years or younger. The distribution of the other datasets remains unknown because their details have not been published or they consist of data from multiple sources. It should be noted that the HF Lung dataset includes data from only 18 participants, as the remaining 261 data points are missing, according to the original paper. Figure 6 shows the segmented age distribution for the SPRSound and Circor 2022 datasets. The age categories in the Circor 2022 dataset are based on the pediatric terminology provided by the National Institute of Child Health and Human Development (NICHD).

B.2 AUSCULTATION POSITION

In our benchmark, three distinct types of data (heart sounds, lung sounds, and bowel sounds) are utilized. Below, we summarize and describe the auscultation positions used by different heart sound

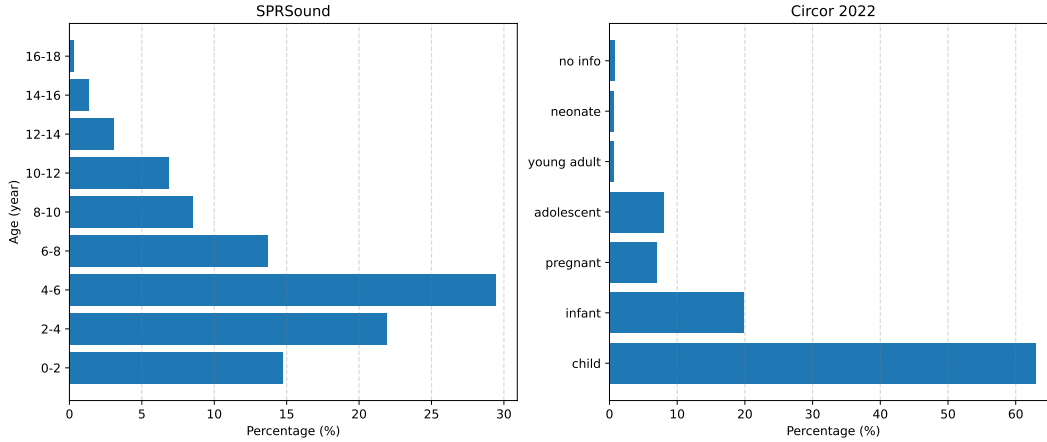


Figure 6: Segmented age distribution of the SPRSound dataset (left) and the Circor 2022 dataset (right).

and lung sound datasets when collecting data. As shown in Table 11, the number of auscultation positions for each heart sound dataset, along with the corresponding diagrams, is provided. The following section offers a detailed description of the auscultation positions used in the different datasets.

Dataset	Sound Type	Auscultation positions	Subfigure	Comment
SPRSound	L	4	(a)	
HF Lung	L	8	(d)	
ICBHI 2017	L	6	(e)	It is collected from two different sources.
Lung Sound	L	10	(c)	
RespiratoryDatabase@TR	L+H	16	(f)	4 channels for heart sounds and 12 channels for lung sounds.
Korean	H	-	-	It is collected from different sources, and there is no fixed auscultation position.
Cinc 2016	H	-	-	It is a collection of 9 heart sound datasets, without a unified standard.
Circor 2022	H	4	(b)	
HSDReport	H	5	-	

Table 11: Auscultation positions of different datasets and their corresponding diagram labels.

SPRSound. The respiratory sounds were recorded at four locations on the back, including left posterior, left lateral, right posterior, and right lateral as shown in Figure 7(a).

HF Lung. As shown in Figure 7(d), there are eight auscultation positions (L1-L8) are defined as follows: L1: the second intercostal space (ICS) on the right midclavicular line (MCL); L2: the fifth ICS on the right MCL; L3: the fourth ICS on the right midaxillary line (MAL); L4: the tenth ICS on the right MAL; L5: the second ICS on the left MCL; L6: the fifth ICS on the left MCL; L7: the fourth ICS on the left MAL; L8: the tenth ICS on the left MAL.

ICBHI 2017. There are two sources of data, the first source is from the Respiratory Research and Rehabilitation Laboratory of the School of Health Sciences, University of Aveiro. Sounds were recorded from the trachea and six chest locations: left and right front, back and side. The second source is from Aristotle University of Thessaloniki. Sounds were sequentially collected from six chest locations, as shown in Figure 7(e), with a digital stethoscope (WelchAllyn Meditron Master Elite Plus Stethoscope Model 5079-400 or 3M Littmann 3200).

Lung Sound. The data were collected by placing the stethoscope on various regions of the chest referred to as zones. Figure 7(c) illustrates the approximate boundaries of the chest zones. The chest zones are defined as follows: 1. Upper zone: located in the region under the clavicles and above the cardiac silhouette (i.e., the superior aspect of the hilum). Sometimes this region includes the apical zone, which is located above the inferior margin of clavicles. 2. Middle zone: located in the region

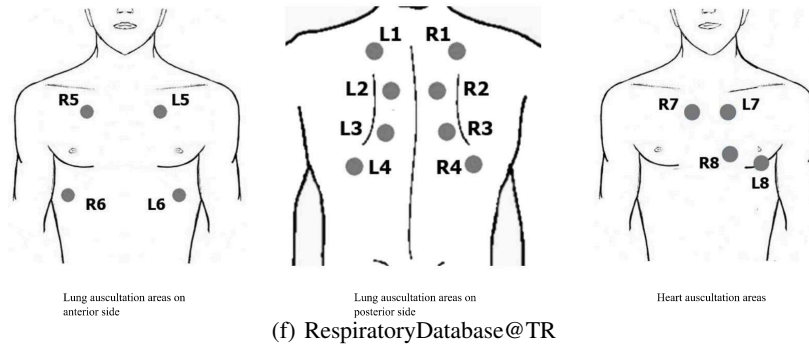
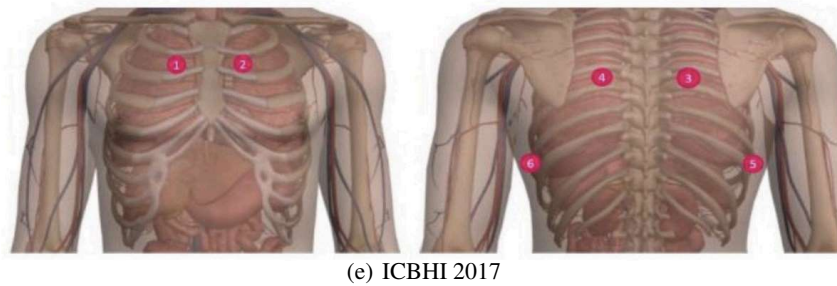
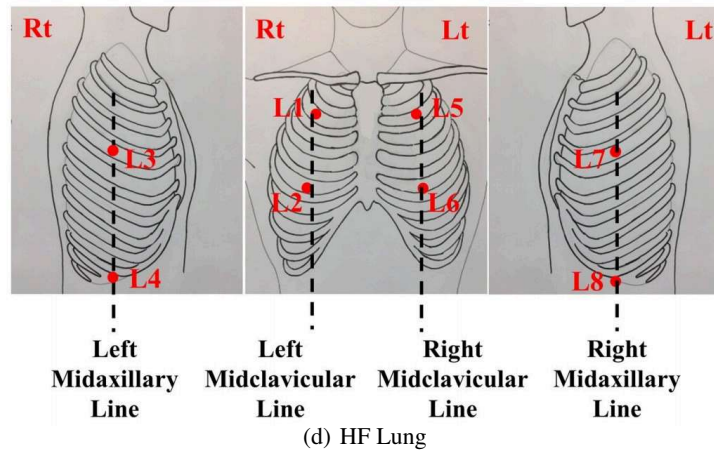
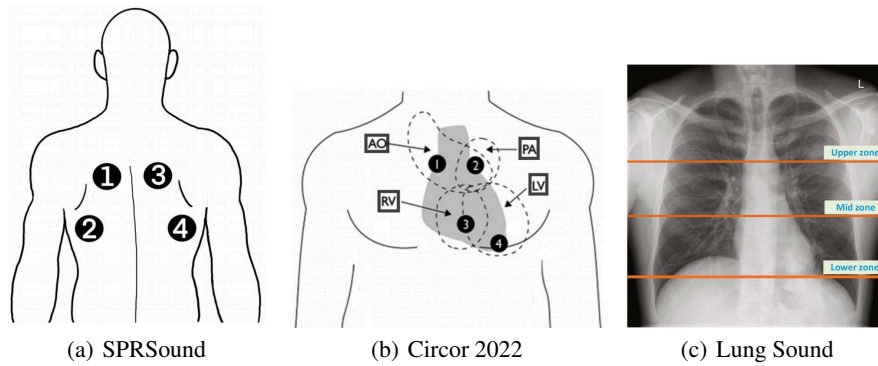


Figure 7: Schematic diagram of auscultation positions for different datasets. These subfigures are all from the corresponding papers. The Circor 2022 (Oliveira et al., 2021) dataset is a heart sound dataset, RD@TR (Altan et al., 2017) contains heart sound and lung sound data, and the remaining datasets (SPRSound (Zhang et al., 2022), Lung Sound (Fraiwan et al., 2021), HF Lung (Hsu et al., 2021a) and ICBHI 2017 Rocha et al. (2019)) are all composed of lung sound data.

between the superior and inferior aspect of the hilum. 3. Lower zone: located in the region enclosed by the inferior aspect of the hilum and the hemidiaphragm. Data from 10 chest zones were finally collected: anterior left upper, anterior right upper, anterior right middle, anterior right lower, posterior left lower, posterior left middle, posterior left upper, posterior right lower, posterior right middle and posterior right upper.

RespiratoryDatabase@TR. There are 16 channels in total, 4 channels for heart sounds focusing on the aorta, pulmonary artery, tricuspid valve, and mitral valve areas. 12 channels for lung sounds focusing on the upper lung, middle lung, lower lung, and costophrenic angle areas on the posterior and anterior sides of the chest. As shown in figure 7(f), the chest auscultation areas used in the physical examination include the posterior upper lung (L1-R1), posterior middle lung (L2-R2), posterior lower lung (L3-R3), posterior costophrenic angle lung (L5-R5), and anterior lower lung (L6-R6) on the left (L) and right (R) sides of the patient. The left image illustrates the chest auscultation areas on the anterior chest wall, while the middle image shows the posterior (back) chest auscultation areas. Heart auscultation is performed at four distinct locations: the aorta (R7), pulmonary artery (L7), tricuspid valve (R8), and mitral valve (L8) areas. The cardiac auscultation areas are shown in the right figure of Figure 7(f).

Circor 2022. Normal heart sounds are primarily generated by the vibrations of cardiac valves as they open and close during each cardiac cycle and the turbulence of blood into the arteries. The anatomical positions of heart valves relative to the chest wall determine the optimal auscultation position. Consequently, the stethoscope should be placed at the following positions for auscultation, as illustrated in Figure 7(b): Aortic valve (1): second intercostal space, right sternal border; Pulmonary valve (2): second intercostal space, left sternal border; Tricuspid valve (3): left lower sternal border; Mitral valve (4): fifth intercostal space, midclavicular line (cardiac apex).

HSDReport. The auscultation protocol consists of recordings from five body sites: aortic region (right 2nd intercostal space), pulmonic region (left 2nd intercostal space, parasternal), Erb’s point (left 3rd intercostal space, also known as the left lower sternal border), tricuspid region (left 4th intercostal space, parasternal), mitral region (left 5th intercostal space, midclavicular).

B.3 SOUND SPECTROGRAM

As shown in Figure 8, two different audio samples were selected from the Circor 2022, Lung Sound, and Bowel Sound datasets. For each sample, 64-dimensional Mel spectrogram features were extracted to facilitate a visual comparison of the differences between the Mel features of these three types of sounds. Generally, bowel sound recordings are relatively short, averaging around 2 seconds, followed by lung sound recordings at approximately 20 seconds. In contrast, heart sound data can be significantly longer, exceeding 60 seconds. During the training phase, slice processing was applied to handle varying recording lengths.

C DOWNSTREAM TASK DESCRIPTION

Here, we provide a detailed description of all 16 tasks defined in the benchmark. These tasks are organized into four categories:

- **Binary Classification (Tasks 3, 13, 14, 15):** Tasks that require predicting a binary outcome (normal/abnormal) from an audio recording.
- **Multi-Class Classification (Tasks 1-2, 4-9, 11-12):** The tasks involve classifying an audio recording into one or multiple classes of several predefined categories.
- **Multi-Label Classification (Task 10):** The task involves classifying an audio recording into one of several predefined categories.
- **Regression (Task 16):** The task of predicting continuous values from audio data, such as the count of bowel sounds.

Below is a description of the downstream tasks performed using different datasets.

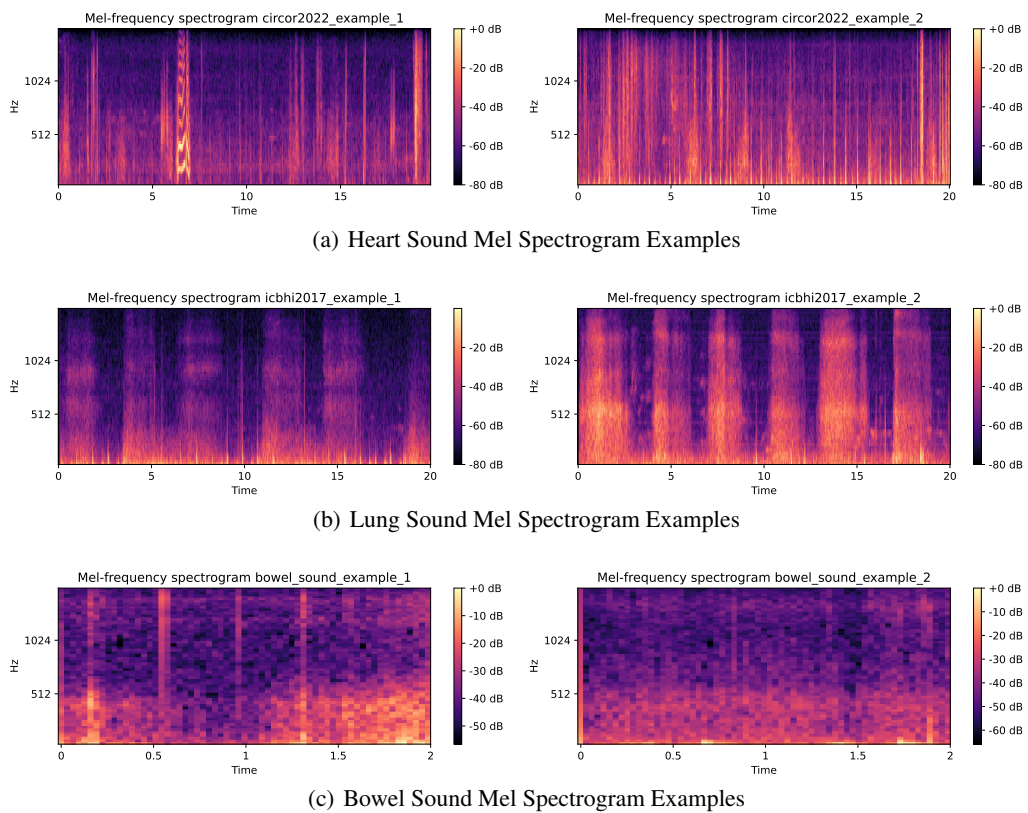


Figure 8: Mel spectrograms of heart sounds, lung sounds, and bowel sounds, using audio from the Circor 2022, ICBHI 2017, and Bowel Sound datasets as examples, respectively.

Task 1: SPRSound_MC_Record. Task 1 involves ternary classification at the record level, with the objective of categorizing respiratory sound records into three classes: Normal, Adventitious, and Poor Quality.

Task 2: SPRSound_MC_Record. Task 2 involves multi-class classification at the record level, with the objective of categorizing respiratory sound records into one of five classes: Normal, CAS, DAS, CAS & DAS, or Poor Quality.

Task 3: HF_Lung_BC_LungSound. Task 3 is a binary classification task aimed at classifying respiratory sound events as Normal or Abnormal.

Task 4: HF_Lung_MC_LungSound. Task 4 is a four-class classification task aimed at classifying respiratory audio into four respiratory cycles: Inhalation, Exhalation, CAS, and DAS. A respiratory cycle refers to the sequence of events during which a person inhales (inspiration) and exhales (expiration) a given volume of air through the respiratory system.

Task 5: HF_Lung_MC_LungSound. Task 5 is a six-class classification task. Building upon Task 4, the categories CAS and DAS are further subdivided to classify respiratory audio into the following six classes: Inhalation, Exhalation, Wheeze, Stridor, Rhonchi, and Crackle.

Task 6: LungSound_MC_LungSound. Task 6 is a seven-class classification task, aiming to classify audio into the following categories based on breathing cycles: Normal, Crepitation, Wheeze, Crackle, Bronchi, Wheeze & Crackle, and Bronchi & Crackle.

Task 7: ICBHI2017_MC_LungSound. Task 7 is a four-class lung sound classification task, aiming to classify respiratory events into four types of respiratory cycles: Normal, Crackle, Wheeze, and Crackle & Wheeze.

Task 8: Circor2022_MC_Murmur. Task 8 is a three-class classification task, aiming to classify heart murmurs into three categories: Present, Absent, and Unknown.

Task 9: ICBHI2017_MC_Disease. Task 9 is a six-category classification task for lung diseases, where the goal is to predict the presence of six conditions based on the entire audio: Bronchiectasis, Bronchiolitis, COPD, Pneumonia, URTI, and Healthy.

Task 10: LungSound_ML_Disease. Task 10 is a disease detection task involving eight categories, aiming to detect the presence of the following conditions based on audio: Normal, Asthma, Pneumonia, COPD, Bronchitis (BRON), Heart Failure, Lung Fibrosis, and Pleural Effusion.

Task 11: RD@TR_MC_Disease. Task 11 is a five-class classification task that categorizes the data into COPD severity levels ranging from 0 to 4 based on audio. The goal of this task is to predict the severity of COPD using lung sounds.

Task 12: Korean_MC_Disease. Task 12 is a five-class classification task that aims to detect the presence of heart diseases based on audio, including Normal (N), Aortic Stenosis (AS), Mitral Regurgitation (MR), Mitral Stenosis (MS), and Mitral valve prolapse (MVP).

Task 13: Cinc2016_BC_Disease. Task 13 is a binary classification task that aims to classify sound events as Normal or Abnormal.

Task 14: Circor2022_BC_Disease. Task 14 is a binary classification task that aims to classify sounds as normal or abnormal for detecting cardiac abnormalities.

Task 15: HSDReport_BC_Disease. Task 15 is a binary classification task that aims to classify cardiac sound events as Normal or Abnormal.

Task 16: BowelSound_R_Count. Task 16 is a regression task aimed at assessing the frequency of specific intestinal activities or patterns by counting the occurrence of bowel sounds in the recordings.

D IMPLEMENTATION DETAILS

D.1 PRETRAINING

Data Processing We pre-train our model using a combination of 11 datasets as described in Table 1. We apply validation with the validation sets of the datasets (e.g. SPRSound, HF Lung, ICBHI 2017, and Bowel Sound). For those datasets that do not have an existing validation set, we randomly split 10% of the data to serve for validation. To adapt to the varied lengths of recordings, we adopt random cropping for each audio and feed them to the pertaining. according to the minimum duration of the recordings for each dataset, different crop lengths are set. Specifically, the cropped length for Korean and Bowel Sound is set as 320 ms, while it is 640 ms for others. Additionally, as a usual augmentation technique, we adjust the loudness of the recording (Schlüter & Grill, 2015) with a random scale factor ranging from 0.9 to 1.1. Moreover, SpecAugment (Park et al., 2019) is also adopted.

Contrastive Learning-based Method The target of our method is to guide the model to distinguish the source of audio segments, where the two segments from the same spectrogram are regarded as a positive pair, otherwise negative pairs. Given two segments x and x' , the features will first be extracted with an encoder $f(\cdot)$ from them, and then a projector $g(\cdot)$ will map the features into a lower dimensional space to obtain the final representation. To improve the quality and discriminative power of the learned representations, an extra linear layer W is added on top of the whole model for the positive/negative anchor x' . Then the bilinear similarity $s(\cdot)$ is calculated as

$$s(x, x') = g(f(x))^T W g(f(x')). \quad (1)$$

Given a batch of samples $\mathcal{X} = \{x_1, x_2, \dots, x_N\}$, the bilinear similarity will be calculated for each sample pair, where the positive anchor of x_i is represented as x^+ , and the negative distractors are $\mathcal{X}^-(x_i) = \{x^- | x^- \neq x^+, \forall x^- \in \mathcal{X}\}$. In this way, the loss function for a batch can be treated as a multi-class classification problem and formulated as

$$\mathcal{L} = -\frac{1}{N} \sum_{i=1}^N \log \frac{\exp(s(x_i, x^+))}{\sum_{x^- \in \mathcal{X}^-(x_i) \cup \{x^+\}} \exp(s(x_i, x^-))}. \quad (2)$$

D.2 BENCHMARKING

Data Processing In the evaluation stage, we adopt the validation set of the pretraining stage as the test set, which is always held out for pretraining and downstream fine-tuning. Considering the varied lengths of different recordings even within the same dataset, each audio in the training set is chunked and padded into the same length. Specifically, each recording of all the datasets is chunked into 8s except for T14 (Korean dataset) and T18 (Bowel Sound dataset). We choose 8s to satisfy the input requirements of different models as shown in xx. As for the Korean and Bowel Sound datasets, the maximum durations are set as 4s and 2s respectively because their recordings are rather short as demonstrated in Table 1.

Baselines Within our benchmark of downstream tasks, we have chosen four pre-trained acoustic models to compare with our models: OPERA-CT, CLAP, AudioMAE, and PANN. The official implementations for each baseline are strictly followed. For example, we resampled all of the recordings with 44.1 kHz and 32 kHz for CLAP and PANN respectively.

E PRETRAINING RESULTS

E.1 PRETRAINING LOSS & ACCURACY

We exhibit the loss and accuracy during the pretraining process. As Figure 9 shows, the training loss of different subsets of the data converges at different speeds and levels, as well as the accuracy rate is gradually increasing. Similarly, Figure 10 presents the evolution of the validation loss and accuracy

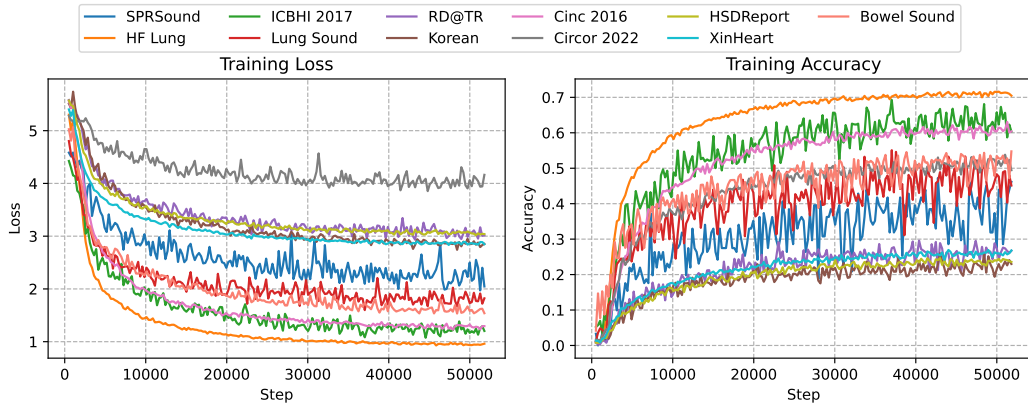


Figure 9: Training loss and contrastive instance discrimination accuracy of our model during the pretraining process.

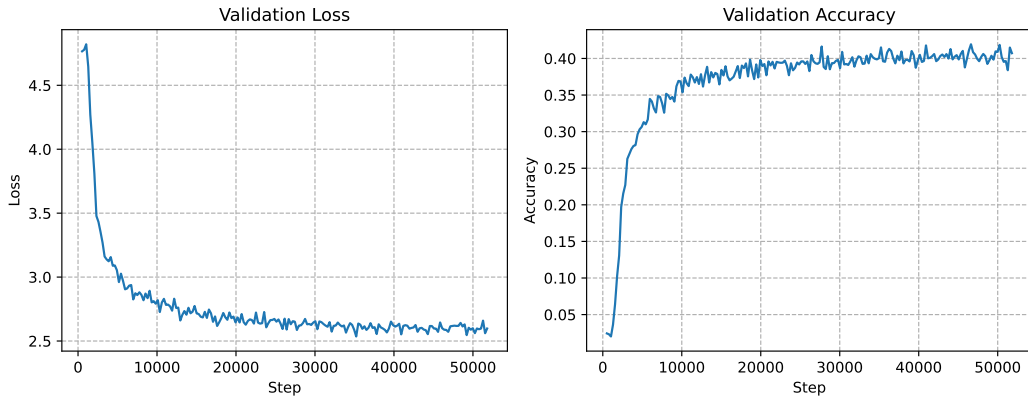


Figure 10: Validation loss and contrastive instance discrimination accuracy of our model during the pretraining process.

on the combined subset of all the data resources, which also demonstrates a continued decay until convergence.

The varied convergence speed is relevant to the heterogeneity in data quality and modality. Meanwhile, the degree of task difficulty (e.g., the crop length and batch size) also affects the convergence level. In general, the longer the crop length is and the smaller the batch size is, the easier the discriminative task will be, which leads to lower training loss but worse model generalizability.

E.2 EMBEDDING DISTRIBUTION

To clarify the discriminative capability of the features extracted by our model, we visualize the T-SNE distribution as shown in Figure 11. Specifically, 8 segments are randomly cropped from each recording, and 5 samples for each dataset are visualized. As depicted in Figure 11, the segments from the same recording are close to each other while far away from others in the embedding space, which reveals that our model can capture the underlying homogeneous characteristics of the same recording despite the variance introduced by random cropping.

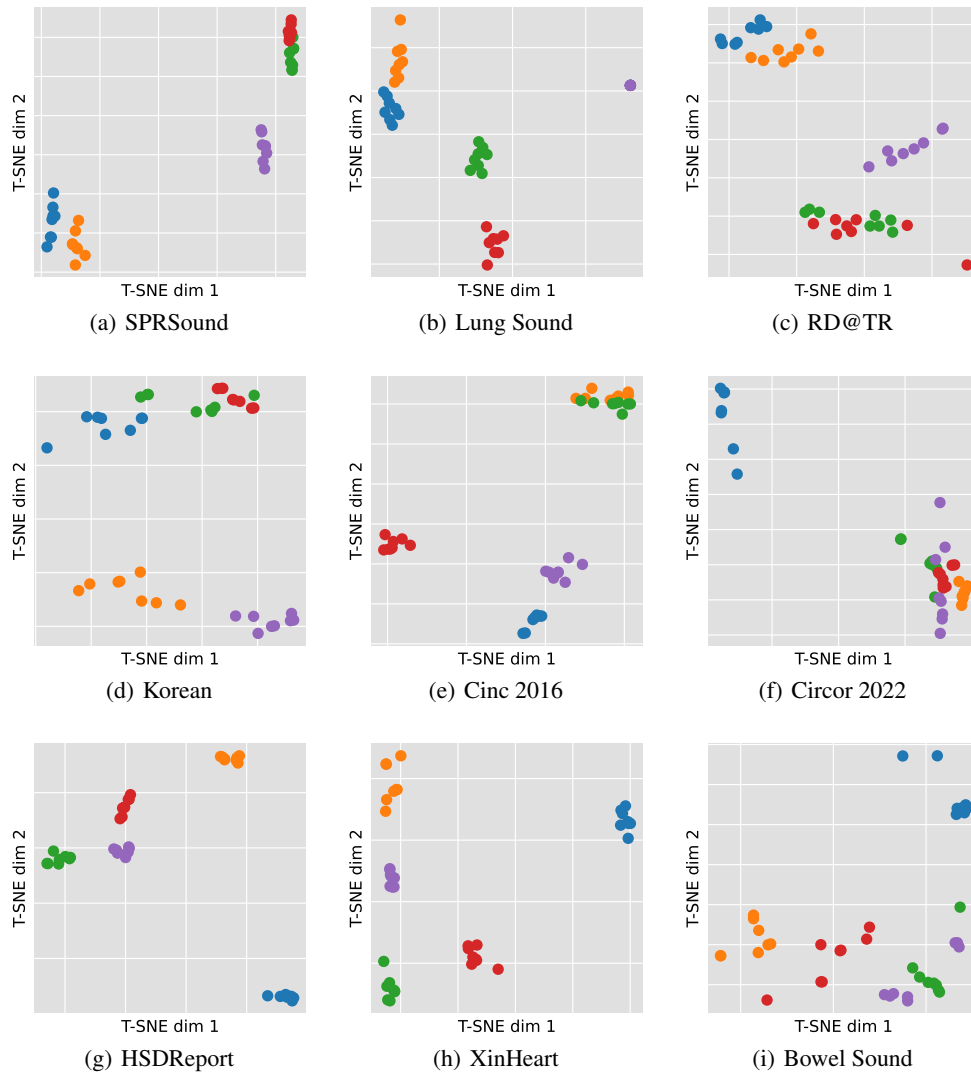


Figure 11: Biodimensional T-SNE visualizations results of the features of our model on the validation set of different datasets. Each dot represents a segment, and the dots with the same color denote that they are from the same recording.

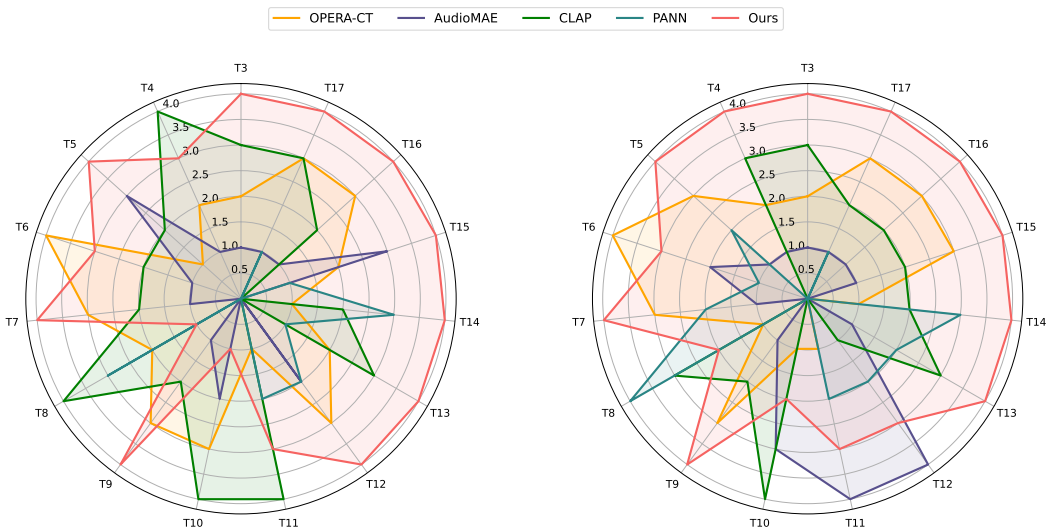


Figure 12: Radar plot of reciprocal ranks of Macro-F1 and Micro-F1 scores for classification tasks respectively.

F ADDITIONAL EVALUATION RESULTS

F.1 PERFORMANCE RADAR PLOT

Apart from the mean reciprocal ranks tasks depicted in Table 6, we demonstrate the reciprocal ranks of all the classification tasks (T3-T17) which is detailed in Figure 12.